

Complexes of Vitamin B₆.

XVII*. Crystal Structure and Molecular Orbital Calculations of the Dichloro-bis-pyridoxol Palladium(II) Complex

M. A. MAKHYOUN, N. A. AL-SALEM and M. S. EL-EZABY**

Chemistry Department, Kuwait University, Kuwait

Received April 26, 1985

Abstract

The structure of dichloro-bis-pyridoxol palladium(II) complex $[\text{PdCl}_2(\text{C}_8\text{H}_{11}\text{O}_3\text{N})_2]$ has been determined from three dimensional X-ray data collection. The complex crystallizes in the monoclinic space group $P2_1/c$ with $Z = 2$ and cell dimensions $a = 5.265(3)$, $b = 17.250(6)$, $c = 10.253(6)$ Å, $\beta = 95.40(2)^\circ$. The structure was refined to a final R factor of 0.060 for 1813 reflections with $F \geq 3\sigma(F)$. The palladium atom lies in a symmetry center of inversion in a square plane coordinated to two chlorine atoms and two pyridine nitrogen atoms. Charge distributions and bond order matrix calculated from ARCANA-MO are given.

Introduction

Pd(II) complexes with the compounds of vitamin B₆ have been recently reported to inhibit the growth as well as the biosynthesis of RNA, DNA and protein of *E. coli* B-766. They also inhibited the incorporation of ³H-thymidine as well as ¹⁴C-leucine in the DNA and protein of liver cell cultures (BL8L). In addition, they inhibited the cell division of Walker-S-Celles and human lymphocytes [1]. Photoacoustic spectral measurements showed that the complexes were bound to DNA of *E. coli* and were present only in the kidney of treated mice [1].

In order to confirm the mode of attachment to the DNA, a prior structure elucidation of Pd(II) complexes with vitamin B₆ compounds should be made.

The molecular structure of vitamin B₆ compounds and their metal complexes have been the subject for many investigations [2–6]. None of the metal complexes studied so far involved a coordination through the ring nitrogen atom, but rather through the phenolic oxygen.

The present paper reports the crystal structure for Pd(II) pyridoxol complex together with a semi-empirical MO calculation of the bond order and charge distributions in this complex.

Experimental

The preparation of Pd(II) complex with pyridoxol (P) has been reported previously [1]. An aqueous solution of 10 mmol of pyridoxol hydrochloride (P·HCl) and 2 mmol of H₂PdCl₄ has been adjusted to pH ~ 4.0 and stirred at room temperature for 1 h. The solution was left overnight. The resulting crystalline yellow product was filtered off and washed with water, then was dried under vacuum. The composition was compatible with the formula Pd(PH)₂Cl₂.

X-ray Data Collection[†]

A yellow needle crystal having approximate dimensions of 0.10 × 0.10 × 0.30 mm was mounted on a glass fiber in a random orientation. Preliminary examination and data collection were performed with Mo K α radiation ($\lambda = 0.71073$ Å) on an Enraf-Nonius CAD4 computer controlled kappa axis diffractometer equipped with a graphite crystal, incident beam monochromator.

Cell constants and an orientation matrix for data collection were obtained from least-squares refinement, using the setting angles of 25 reflections in the range $4 < \theta < 13^\circ$, measured by the computer controlled diagonal slit method of centering. The monoclinic cell parameters are: $a = 5.265(3)$, $b = 17.250(6)$, $c = 10.253(6)$, $\beta = 95.40(2)^\circ$, $V = 927.1$ Å³, for $Z = 2$, $F_w = 515.67$ and $D_c = 1.85$ g/cm³. As a check on crystal quality, omega scans of several intense reflections were measured: the width at half-height was 0.20° with a take-off angle of 2.8° , indicating good crystal quality. From the systematic absences of: $h0l$, $l =$

*Part XVI. Kinetics and Reaction Mechanism of Fe(III) Complexes with Pyridoxal-5'-Phosphate; see ref. 22.

**Author to whom correspondence should be addressed.

[†]X-ray data collected by The Molecular Structure Corporation, Tex., U.S.A., 1982.

$2n + 1$ and $0k0$, $k = 2n + 1$ and from subsequent least-squares refinement, the space group was determined to be $P2_1/c$ (#14).

The data were collected at a temperature of $23 \pm 1^\circ\text{C}$ using the ω - θ scan technique. The scan rate varied from 2 to $20^\circ/\text{min}$ (in ω). The variable scan rate allows rapid data collection for intense reflections where a fast scan rate is used and assures good counting statistics for weak reflections where a slow scan rate is used. Data were collected to a maximum 2θ of 60.0° . The scan range (in deg) was determined as a function of θ to correct for the separation of the $K\alpha$ doublet [7]; the scan width was calculated as follows:

$$\theta \text{ scan width} = 0.8 + 0.350 \tan \theta$$

Moving-crystal moving counter background counts were made by scanning an additional 25% above and below this range. Thus the ratio of peak counting time to background counting time was 2:1. The counter aperture was also adjusted as a function of θ . The horizontal aperture width ranged from 2.0 to 2.6 mm; the vertical aperture was set at 2.0 mm. The diameter of the incident beam collimator was 0.7 mm and the crystal to detector distance was 21 cm. For intense reflections an attenuator was automatically inserted in front of the detector; the attenuator factor was 20.7.

Data Reduction

A total of 2919 reflections were collected, of which 2705 were unique and not systematically absent. As a check on crystal and electronic stability 3 representative reflections were measured every 41 min. The intensities of these standards remained constant within experimental error throughout data collection. No decay correction was applied.

Lorentz and polarization corrections were applied to the data. The linear absorption coefficient is 13.1 cm^{-1} for Mo $K\alpha$ radiation. An empirical absorption correction based on a series of psi-scans was applied to the data. Relative transmission coefficients ranged from 0.667 to 0.994 with an average value of 0.801. An extinction correction was not necessary.

Structure Solution and Refinement

The structure was solved using the Patterson heavy-atom method which revealed the positions of 2 atoms. The remaining atoms were located in succeeding difference Fourier syntheses. Hydrogen atoms were located and their positions and isotropic thermal parameters were refined. The structure was refined in full-matrix least-squares where the function minimized was $\sum w(|F_o| - |F_c|)^2$ and the weight (w) = $4F_o^2/\sigma^2(F_o^2)$.

The standard deviation on intensities, $\sigma(F_o^2)$, is defined as follows:

$$\sigma^2(F_o^2) = [S^2(C + R^2B) + (pF_o^2)^2]/Lp^2$$

where S is the scan rate, C is the total integrated peak count, R is the ratio of scan time to background counting time, B is the total background count, Lp is the Lorentz-polarization factor and the parameter p is a factor introduced to downweight intense reflections. Here p was set to 0.050.

Scattering factors were taken from Cromer and Waber [8]. Anomalous dispersion effects were included in F_c [9]: the values for $\Delta f'$ and $\Delta f''$ were those of Cromer [10]. Only the 1813 reflections having intensities greater than 3.0 times their standard deviation were used in the refinements. The final cycle of refinement included 168 variable parameters and converged (largest parameter shift was 0.39 times its e.s.d.) with unweighted and weighted agreement factors of:

$$R = \sum |F_o| - |F_c| / \sum |F_o| = 0.051$$

$$R_w = \text{SQRT}(\sum w(|F_o| - |F_c|)^2 / \sum w F_o^2) = 0.060$$

The standard deviation of an observation of unit weight was 1.63. The highest peak in the final difference Fourier had a height of $2.36 \text{ e}/\text{\AA}^3$ with an estimated error based on ΔF [11] of 0.18. Plots of $\sum w(|F_o| - |F_c|)^2$ vs. $|F_o|$, reflection order in data collection, $\sin \theta/\lambda$, and various classes of indices showed no unusual trends.

All calculations were performed on a PDP-11/60 computer using the Enraf-Nonius Structure Determination Package as well as private program of Molecular Structure Corporation.

Method of Calculations

ARCANA is a semiempirical charge self-consistent method developed by Cusachs and Corrington [12, 13]. It was applied successfully to organic and inorganic molecules [14, 15]. The same approach [13] has been also applied on dichloro bis-pyridoxol palladium(II) complex (132 basis functions). The method is summarized as follows:

Each valence atomic orbital has been assigned a set of parameters, these are:

A : Valence state ionization potential (VSIP).

B : Change of the VSIP as a function of charge.

R_i : $1/\langle r^{-1} \rangle$ expectation value.

Z and n : exponent and principle quantum number of Slater type orbital, respectively, optimized for overlap.

The parameters selected for this calculation are given in Table VIII.

The method is based upon the solution of the eigenvalue equation:

$$\epsilon = C^+FC$$

where,

$$(i\epsilon A) F_{ii} = \bar{H}_{ii} + \sum_{B \neq A} (-Z_B \langle i|1/r_B|i \rangle) + \sum_{k\epsilon B} \sum_{l\epsilon B} \langle ii|kl \rangle P_{kl}$$

$$(i,j\epsilon A) F_{ij} = \sum_{B \neq A} (-Z_B \langle i|1/r_B|j \rangle) + \sum_{K\epsilon B} \langle ij|kk \rangle P_{ij}$$

$$(p\epsilon A, q\epsilon B) F_{pq} = \bar{H}_{pq}$$

where A and B denote atoms, while i,j,k,l,p,q denote orbitals. $\bar{H} = S^{-1/2} H S^{-1/2}$; $H_{ii} = -A_i - B_i Q_A$; $H_{ij} = (2 - |S_{ij}|) S_{ij} (H_{ii} + H_{jj})/2$; S: overlap matrix; P: population matrix (Lowdin basis); Q: atomic charge (Lowdin basis).

The integrals $\langle i|1/r_B|j \rangle$ and $\langle ii|kl \rangle$ are calculated according to the method described in ref. 13. Two configurations of the complex were calculated; the equilibrium configuration (established from X-ray data) and the symmetric configuration (see 'Discussion').

Discussion

Figure 1 shows the structure of the complex and the atom numbering scheme. The positional, thermal and general temperature factors are listed in Tables I and II. In addition, bond distances and bond angles are given in Tables II-V. The vitamin B₆ compounds and their metal complexes have the tendency to form the zwitterion structure [6], in our case the palladium ion prefers the ring nitrogen site for coordination thus destroying the zwitterion structure

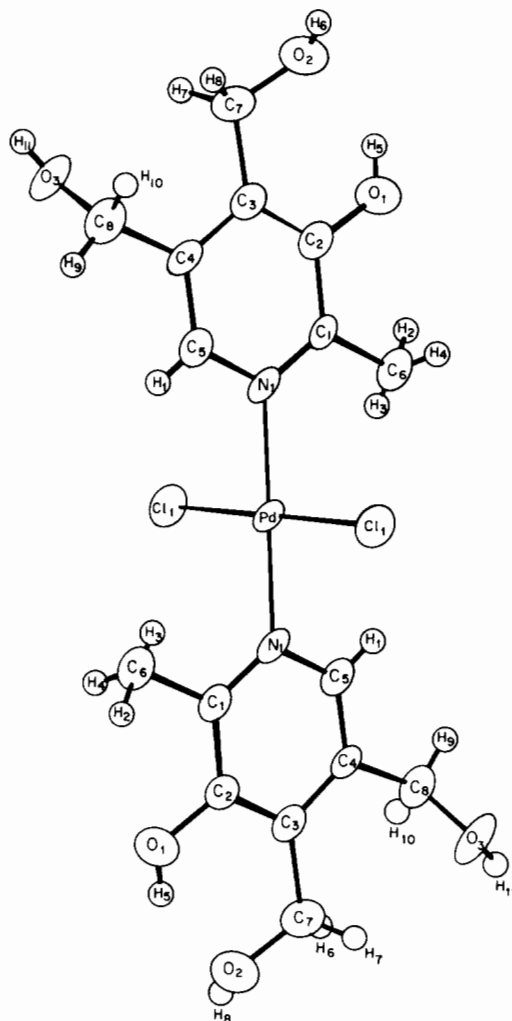


Fig. 1. Complex structure and atom labelling.

TABLE I. Positional and Thermal Parameters and their e.s.d.^a

Atom	x	y	z	$\beta_{1,1}$	$\beta_{2,2}$	$\beta_{3,3}$	$\beta_{1,2}$	$\beta_{1,3}$	$\beta_{2,3}$
Pd	0.000(0)	0.0000(0)	0.0000(0)	0.0272(1)	0.00095(1)	0.00559(3)	-0.0004(1)	0.0065(1)	0.00042(5)
Cl1	0.1985(3)	-0.10641(8)	-0.0820(1)	0.0399(5)	0.00172(3)	0.0091(1)	0.0038(2)	0.0114(4)	-0.0004(1)
O1	-0.2322(8)	0.0807(3)	-0.4962(4)	0.048(2)	0.0036(2)	0.0068(4)	-0.0075(9)	-0.005(1)	0.0019(4)
O2	0.0062(8)	0.1842(3)	-0.6128(4)	0.043(2)	0.0037(2)	0.0069(3)	-0.0014(9)	0.008(1)	0.0021(4)
O3	0.4028(7)	0.2935(2)	-0.2613(4)	0.043(1)	0.0013(1)	0.0134(4)	-0.0024(7)	0.023(1)	0.0002(4)
N1	0.0464(8)	0.0605(2)	-0.1658(4)	0.031(1)	0.0008(1)	0.0067(3)	-0.0002(7)	0.008(1)	0.0004(3)
C1	-0.1049(9)	0.0498(3)	-0.2776(5)	0.026(2)	0.0011(1)	0.0069(4)	-0.0011(8)	0.006(1)	-0.0003(4)
C2	-0.0664(10)	0.0951(3)	-0.3875(5)	0.029(2)	0.0015(1)	0.0066(4)	0.0009(9)	0.0004(1)	0.0004(4)
C3	0.1194(9)	0.1513(3)	-0.3833(4)	0.030(2)	0.0013(1)	0.0064(4)	0.0004(8)	0.010(1)	0.0001(4)
C4	0.2785(9)	0.1594(3)	-0.2652(5)	0.026(2)	0.0010(1)	0.0073(4)	0.0000(8)	0.008(1)	0.0008(4)
C5	0.2331(9)	0.1142(3)	-0.1610(5)	0.025(2)	0.0014(1)	0.0074(4)	-0.0012(8)	0.004(1)	-0.0002(4)
C6	-0.3095(11)	-0.0096(3)	-0.2841(6)	0.032(2)	0.0020(2)	0.0094(5)	-0.0036(10)	0.001(2)	0.0004(5)
C7	0.1545(12)	0.2052(3)	-0.4963(5)	0.051(3)	0.0026(2)	0.0076(5)	-0.0048(13)	0.011(2)	0.0024(5)
C8	0.4989(10)	0.2164(3)	-0.2504(6)	0.030(2)	0.0018(2)	0.0100(5)	-0.0015(9)	0.010(2)	0.0000(5)

(continued overleaf)

TABLE I. (continued)

Atom	x	y	z	B_{A^2}	Atom	x	y	z	B_{A^2}
H1	0.315(9)	0.121(3)	-0.089(5)	3(1)	H7	0.134(18)	0.257(6)	-0.474(9)	10(3)
H2	-0.438(14)	0.010(4)	-0.344(7)	6(2)	H8	0.097(15)	0.177(5)	-0.662(7)	8(2)
H3	-0.331(16)	-0.010(5)	-0.225(8)	7(2)	H9	0.605(10)	0.210(3)	-0.173(5)	3(1)
H4	-0.300(15)	-0.038(5)	-0.339(7)	8(2)	H10	0.585(11)	0.207(4)	-0.310(6)	5(2)
H5	-0.184(11)	0.102(4)	-0.556(6)	4(1)	H11	0.531(12)	0.316(4)	-0.286(6)	6(2)
H6	0.320(9)	0.214(3)	-0.508(5)	3(1)					

^aThe form of the anisotropic thermal parameter is: $\exp[-(\beta_{1,1}h^2 + \beta_{2,2}k^2 + \beta_{3,3}l^2 + \beta_{1,2}hk + \beta_{1,3}hl + \beta_{2,3}kl)]$. Estimated standard deviations in the least significant digits are shown in parentheses.

TABLE II. General Temperature Factor Expressions^a

Name	$B_{1,1}$	$B_{2,2}$	$B_{3,3}$	$B_{1,2}$	$B_{1,3}$	$B_{2,3}$	B_{eq}
Pd	2.99(2)	1.13(1)	2.33(1)	-0.08(2)	0.69(1)	0.15(2)	2.123(7)
Cl1	4.38(5)	2.04(4)	3.79(5)	0.68(4)	1.22(4)	-0.13(4)	2.35(2)
O1	5.2(2)	4.3(2)	2.8(1)	-1.3(2)	-0.5(1)	0.7(1)	4.18(9)
O2	4.7(2)	4.4(2)	2.9(1)	-0.3(2)	0.8(1)	0.7(1)	3.95(9)
O3	4.7(2)	1.6(1)	5.6(2)	-0.4(1)	2.5(1)	0.1(1)	3.82(8)
N1	3.4(2)	1.0(1)	2.8(1)	-0.0(1)	0.9(1)	0.1(1)	2.33(7)
C1	2.9(2)	1.4(1)	2.9(2)	-0.2(1)	0.6(1)	-0.1(1)	2.35(8)
C2	3.2(2)	1.8(2)	2.8(2)	0.2(1)	0.4(2)	0.1(2)	2.59(9)
C3	3.3(2)	1.6(2)	2.7(2)	0.1(2)	1.0(1)	0.0(1)	2.47(9)
C4	2.9(2)	1.2(1)	3.0(2)	0.0(1)	0.8(1)	0.3(1)	2.34(8)
C5	2.8(2)	1.7(2)	3.1(2)	-0.2(2)	0.5(2)	-0.1(2)	2.51(9)
C6	3.5(2)	2.4(2)	3.9(2)	-0.6(2)	0.1(2)	0.1(2)	3.3(1)
C7	5.6(3)	3.1(2)	3.2(2)	-0.9(2)	1.2(2)	0.8(2)	3.9(1)
C8	3.3(2)	2.2(2)	4.2(2)	-0.3(2)	1.1(2)	-0.0(2)	3.2(1)

^aThe form of the anisotropic thermal parameter is: $\exp[-0.25(h^2a^2B_{1,1} + k^2b^2B_{2,2} + l^2c^2B_{3,3} + 2hkabB_{1,2} + 2hlacB_{1,3} + 2klbcB_{2,3})]$ where a , b , and c are reciprocal lattice constants.

TABLE III. Bond Distances (Å) Including Hydrogen Bonds^a

Distance		Distance	
Pd–Cl1	2.310(1)	C2–C3	1.376(6)
Pd–Cl1	2.310(1)	C3–C4	1.414(6)
Pd–N1	2.029(3)	C3–C7	1.510(6)
Pd–N1	2.029(3)	C4–C5	1.363(5)
O1–C2	1.372(5)	O2–O3	2.725(5)
O1–H5	0.78(6)	O3–H8	2.05(7)
O2–C7	1.412(6)	C4–C8	1.517(6)
O2–H8	0.74(7)	C5–H1	0.83(4)
O3–C8	1.424(6)	C6–H2	0.93(7)
O1–O2	2.545(5)	C6–H3	0.63(9)
O2–H5	1.86(6)	C6–H4	0.74(8)
O3–H11	0.84(6)	C7–H6	0.90(5)
N1–C1	1.346(5)	C7–H7	0.93(10)
N1–C5	1.348(5)	C8–H9	0.93(5)
C1–C2	1.402(5)	C8–H10	0.81(5)
C1–C6	1.483(6)		

^aNumbers in parentheses are estimated standard deviations in the least significant digits.

TABLE IV. Bond Angles (°) Including Hydrogen Bond Angles^a

Angle	
Cl1–Pd–Cl1	180.0(0) ^a
Cl1–Pd–N1	90.55(9)
Cl1–Pd–N1	89.45(9)
Cl1–Pd–N1	89.45(9)
Cl1–Pd–N1	90.55(9)
N1–Pd–N1	180.0(0)
C2–O1–H5	109(4)
C7–O2–H8	106(6)
C8–O3–H11	100(4)
Pd–N1–C1	122.3(3)
Pd–N1–C5	117.9(3)
C1–N1–C5	119.8(3)
N1–C1–C2	119.3(4)
N1–C1–C6	120.2(4)
C2–C1–C6	120.5(4)
O1–H5–O2	146(1)

(continued on facing page)

TABLE IV. (continued)

	Angle
O1-C2-C1	115.0(4)
O1-C2-C3	123.3(4)
C1-C2-C3	121.6(4)
C2-C3-C4	117.3(4)
C2-C3-C7	123.2(4)
C4-C3-C7	119.4(4)
C3-C4-C5	118.8(4)
C3-C4-C8	122.4(4)
C5-C4-C8	118.8(4)
N1-C5-C4	123.1(4)
N1-C5-H1	117(3)
C4-C5-H1	120(3)
C1-C6-H2	105(4)
C1-C6-H3	99(8)
C1-C6-H4	113(6)
O2-H8-O3	153(1)
H2-C6-H3	117(9)
H2-C6-H4	81(7)
H3-C6-H4	138(9)
O2-C7-C3	113.2(4)
O2-C7-H6	113(3)
O2-C7-H7	113(6)
C3-C7-H6	113(3)
C3-C7-H7	112(5)
H6-C7-H7	91(6)
O3-C8-C4	109.5(4)
O3-C8-H9	111(3)
O3-C8-H10	111(4)
C4-C8-H9	114(3)
C4-C8-H10	105(4)
H9-C8-H10	106(5)

^aNumbers in parentheses are estimated standard deviations in the least significant digits.

with a shift of the proton to the phenolate oxygen. The valence angles around Pd are close to 90° establishing a square planar coordination. The Pd atom and the two pyridine rings are approximately on the same plane, whereas the Cl-Pd-Cl axis makes an angle of $\sim 78^\circ$ with this plane. On the molecular level the Pd-complex possesses nearly a symmetry belonging to the C_i point group.

Two intramolecular hydrogen bonds and two other intermolecular hydrogen bonds are found in the complex. These are the two, $O_1-H_5 \cdots O_2$ and the two $O_2-H_8 \cdots O'_3$ respectively on both rings, Fig. 1.

The Pd-Cl distance of 2.310 Å is close to the one in $PdCl_4^{-2}$ (2.318 Å) [20]. The bond lengths of the palladium complex in the ligand part are similar to that of pyridoxol. HCl [2], the differences are in the range of ± 0.02 Å except for C_1-C_2 which is longer in the complex by 0.03 Å and the C_8-O_3 which is shorter by ~ 0.07 Å.

TABLE V. Torsional Angles ($^\circ$)

	Angle
Cl1-Pd-N1-C1	78.2
Cl1-Pd-N1-C5	-103.1
H5-O1-C2-C1	-169.9
H5-O1-C2-C3	12.2
H8-O2-C7-C3	-120.5
H8-O2-C7-H6	9.7
H8-O2-C7-H7	111.1
H11-O3-C8-C4	-155.6
H11-O3-C8-H9	78.0
H11-O3-C8-H10	-39.6
Pd-N1-C1-C2	178.3
Pd-N1-C1-C6	-1.9
C5-N1-C1-C2	-0.3
C5-N1-C1-C6	179.5
Pd-N1-C5-C4	-178.5
Pd-N1-C5-H1	-3.1
C1-N1-C5-C4	0.2
C1-N1-C5-H1	175.6
N1-C1-C2-O1	-179.1
N1-C1-C2-C3	-1.2
C6-C1-C2-O1	1.1
C6-C1-C2-C3	179.0
N1-C1-C6-H2	148.7
N1-C1-C6-H3	27.4
N1-C1-C6-H4	-125.3
C2-C1-C6-H2	-31.5
C2-C1-C6-H3	-152.7
C2-C1-C6-H4	54.5
O1-C2-C3-C4	-179.5
O1-C2-C3-C7	2.3
C1-C2-C3-C4	2.8
C1-C2-C3-C7	-175.4
C2-C3-C4-C5	-2.9
C2-C3-C4-C8	176.7
C7-C3-C4-C5	175.4
C7-C3-C4-C8	-4.9
C2-C3-C7-O2	-9.5
C2-C3-C7-H6	-139.8
C2-C3-C7-H7	119.2
C4-C3-C7-O2	172.2
C4-C3-C7-H6	42.0
C4-C3-C7-H7	-59.0
C3-C4-C5-N1	1.5
C3-C4-C5-H1	-173.8
C8-C4-C5-N1	-178.2
C8-C4-C5-H1	6.5
C3-C4-C8-O3	65.4
C3-C4-C8-H9	-170.1
C3-C4-C8-H10	-54.0
C5-C4-C8-O3	-115.0
C5-C4-C8-H9	9.5
C5-C4-C8-H10	125.6

The $C_1-N_1-C_5$ angle is less than the angle observed for protonated pyridine nitrogen by about 5° .

TABLE VI. Intermolecular Contacts up to 3.5 Å Bond Distances (Å)

Distance		Distance		Distance	
Pd–C1	2.974(4) ^a	O1–H10	3.10(6)	C2–C8	3.492(6)
Pd–C5	2.914(4)	O2–O3	3.413(5)	C2–H10	2.82(6)
Pd–C6	3.206(6)	O2–O3	2.725(5)	C3–H2	3.37(7)
Pd–H1	2.87(5)	O2–C4	3.492(5)	C3–H10	3.13(6)
Pd–H3	2.76(9)	O2–C8	3.370(6)	C4–H2	3.12(7)
Cl1–O2	3.480(4)	O2–H4	3.03(9)	C4–H6	3.42(4)
Cl1–O3	3.256(4)	O2–H9	2.81(5)	C4–H7	3.47(9)
Cl1–N1	3.059(3)	O2–H10	3.42(6)	C4–H8	3.19(8)
Cl1–H1	3.37(5)	O2–H11	2.93(6)	C5–H2	3.22(7)
Cl1–H1	2.98(4)	O2–H11	3.42(6)	C5–H3	3.25(9)
Cl1–H3	3.42(8)	O3–C6	3.470(6)	C5–H6	3.37(5)
Cl1–H7	3.03(10)	O3–C7	3.124(6)	C5–H7	3.02(9)
Cl1–H8	3.17(7)	O3–H3	3.41(9)	C6–H5	3.39(6)
Cl1–H9	3.26(5)	O3–H4	3.15(8)	C6–H8	3.17(8)
Cl1–H11	2.45(6)	O3–H5	3.40(6)	C6–H11	3.32(7)
O1–C6	3.373(7)	O3–H6	2.68(4)	C7–H1	3.28(5)
O1–H2	2.76(7)	O3–H7	3.50(9)	C7–H4	3.47(9)
O1–H4	2.95(9)	N1–H9	3.47(5)	C7–H9	3.44(5)
O1–H4	3.49(8)	C1–H9	3.38(5)	C8–H6	2.99(4)
O1–H6	3.28(5)	C1–H10	3.16(6)	C8–H8	3.00(8)

^aNumbers in parentheses are estimated standard deviations in the least significant digits.

TABLE VII. Weighted Least-squares Planes. The Equation of the Plane is of the Form: $A*x + B*y + C*z - D = 0$ where A , B , C and D are Constants and x , y and z are Orthogonalized Coordinates

Plane Number	A	B	C	D	Atom	x	y	z	Distance	e.s.d.					
1	-0.8494	-0.3338	-0.4088	0.0000	Atoms in plane										
					Pd	0.0000	0.0000	0.0000	0.000	0.000					
					Cl1	1.1243	-1.8356	-0.8373	0.000	0.001					
					N1	0.4041	1.0438	-1.6919	0.000	0.004					
					Other atoms										
					C1	-0.2845	0.8588	-2.8334	1.113	0.005					
					C5	1.3826	1.9692	-1.6431	-1.160	0.005					
					2	0.6666	-0.6831	-0.2986	0.0667	Atoms in plane					
										N1	0.4041	1.0438	-1.6919	-0.005	0.004
										C1	-0.2845	0.8588	-2.8334	0.003	0.005
C2	0.0242	1.6400	-3.9553	0.010						0.005					
C3	0.9984	2.6104	-3.9125	-0.016						0.005					
C4	1.7225	2.7502	-2.7066	0.011						0.005					
C5	1.3826	1.9692	-1.6431	0.000						0.005					
Other atoms															
Pd	0.0000	0.0000	0.0000	-0.067						0.000					
Cl1	1.1243	-1.8356	-0.8373	2.186						0.001					
C6	-1.3554	-0.1651	-2.9002	0.008						0.006					
O1	-0.7436	1.3918	-5.0647	-0.001						0.004					
C7	1.2927	3.5395	-5.0659	-0.110						0.006					
O2	0.6240	3.1771	-6.2554	0.047						0.004					
C8	2.8686	3.7323	-2.5557	0.059						0.006					
O3	2.3732	5.0629	-2.6668	-1.147	0.004										

(continued on facing page)

TABLE VII. (continued)

Plane Number	A	B	C	D	Atom	x	y	z	Distance	e.s.d.
3	0.8911	-0.4364	-0.1242	0.2362	Atoms in plane					
					C3	0.9984	2.6104	-3.9125	0.000	0.005
					C7	1.2927	3.5395	-5.0659	0.000	0.006
					O3	2.3732	5.0629	-2.6668	0.000	0.004
					Other atoms					
					C2	0.0242	1.6400	-3.9553	-0.439	0.005
					C4	1.7225	2.7502	-2.7066	0.435	0.005

Chi-squared values

Plane number	Chi-squared
1	0.0
2	23.0
3	0.0

Dihedral angles between planes

plane number	Plane Number	Dihedral Angle
1	2	102.5
1	3	124.1
2	3	21.7

TABLE VIII. Parameters used in MO Calculations

		A ^a	B ^d	R _i ^e	Z ^f	n ^f
Pd	5S	7.43 ^b	4.94	2.68	1.04	3
	4d	11.74 ^b	11.89	1.11	1.81	2
Cl	3S	25.26	11.62	1.14	2.24	3
	3P	13.68	10.27	1.29	1.36	2
O	2S	33.2	16.76	0.79	2.19	2
	2P	15.3	14.71	0.90	1.22	1
N	2S	25.56	14.96	0.89	1.88	2
	2P	13.19	13.25	1.0	1.10	1
C	2S	19.54	11.4	1.16	1.72	2
	2P	11.20	10.34	1.28	0.88	1
H	1S	9.0 ^c	18.92	0.70 ^c	1.45 ^c	1

^aRef. 16. ^bVSIP derived from the data in ref. 17. ^cRef. 15. ^d $B = 2/3 (0.73/R_i)$ [13]. ^eRefs. 12, 18. ^fRef. 19.

The results of the MO calculation of the complex and the free pyridoxol* are summarized in Tables IX and X. For the sake of comparison the free ligand was also calculated by the MINDO/3 method [21]. Although the ARCANA and the MINDO/3 have different origins, the charge distribution calculated by the ARCANA (Lowdin basis) and MINDO/3 (Table IX) are relatively close. (except the high charge of nitrogen predicted by the ARCANA-method). On the other hand, atomic charges calculated within

TABLE IX. Self-consistent Charge Distribution

	ARCANA Lowdin population		ARCANA Mulliken population		MINDO/3
	Complex	Free Ligand	Complex	Free Ligand	Free ligand
Pd	0.864	-	1.018	-	-
N	-0.777	-0.576	-0.901	-0.566	-0.182
Cl	-0.166	-	-0.214	-	-
C1	0.249	0.259	0.296	0.305	0.104
C2	0.426	0.420	0.466	0.459	0.305
C3	-0.087	-0.077	-0.088	-0.084	-0.121
C4	-0.232	-0.231	-0.177	-0.176	-0.078
C5	0.450	0.432	0.335	0.341	0.03
C6	0.381	0.376	-0.014	0.057	-0.313
C7	0.548	0.541	0.392	0.410	0.418
C8	0.557	0.551	0.389	0.400	0.350
O1	-0.564	-0.568	-0.331	-0.828	-0.524
O2	-0.534	-0.537	-0.794	-0.789	-0.586
O3	-0.603	-0.606	-0.808	-0.804	-0.514
H1	-0.078	-0.067	0.03	0.033	0.043
H2	-0.162	-0.138	-0.054	-0.043	0.070
H3	-0.096	-0.076	0.014	0.016	0.123
H4	-0.153	-0.143	0.023	0.006	0.159
H5	0.287	0.292	0.487	0.480	0.303
H6	-0.106	-0.101	0.006	0.001	-0.056
H7	-0.091	-0.087	0.014	0.001	-0.059
H8	0.236	0.242	0.441	0.432	0.320
H9	-0.089	-0.086	0.011	0.009	-0.048
H10	-0.116	-0.114	-0.018	-0.02	-0.003
H11	0.289	0.294	0.458	0.447	0.260

*The cartesian coordinates are taken as in the complex.

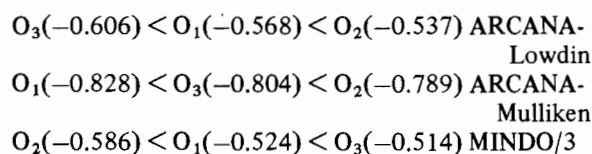
TABLE X. Mulliken Bond Order Matrix.

	ARCANA		MINDO/3 ^a
	Complex	Free ligand	Free ligand
Pd-N	0.154	—	—
Pd-Cl	0.255	—	—
N-Cl	0.531	0.742	0.770
N-C5	0.764	0.961	0.750
C1-C2	1.136	1.114	0.829
C1-C6	1.252	1.208	0.672
C2-C3	1.051	1.072	0.888
C2-O1	0.576	0.569	0.504
C3-C4	0.620	0.680	0.819
C3-C7	0.951	0.941	0.660
C4-C5	1.237	1.165	0.902
C4-C8	0.888	0.893	0.649
C5-H1	0.547	0.582	0.782
C7-O2	0.643	0.636	0.464
C8-O3	0.649	0.640	0.450
O1-H5	0.547	0.485	0.560
O2-H8	0.465	0.474	0.586
O3-H11	0.521	0.529	0.532
O2...H5	0.045	0.047	0.014

$$^a \text{Bond order (A,B)} = \sum_{k \in A} \sum_{l \in B} 2P_{lk} S_{lk}$$

the ARCANA using the Lowdin basis or using the Mulliken approach are quite similar for carbon and hydrogen. The latter approach gives higher negative values for oxygen and nitrogen and it seems that the Lowdin population method for charge is more reasonable.

None of three approaches predicts the same relative order of charge on similar atoms, for example, the result for the net charges for the three oxygen atoms of the free ligand are:



The palladium complex converged with an atomic Lowdin population of $4d^{8.465} 5s^{0.517}$ and a similar Mulliken population of $4d^{8.61} 5s^{0.526}$. It is seen from Tables IX and X that the charge distribution and bond order are different in the complex compared to the free ligand only at the vicinity of the metal center. The coordination of palladium with nitrogen lead to an increase of the net charge on nitrogen and a withdrawal of charge from the N-C₁ and N-C₅ bonds. A polarization effect which seems to be reasonable for a large cation and a polarizable double bond. The charge on palladium is mainly reduced from the coordination of the chloride ions. The low net charges on chlorine atoms indicates a greater covalent bonding.

The calculated bond orders of the free ligand (pyridoxol-HCl) using MINDO/3 method, Table X, are in good agreement with the experimental bond lengths [2].

There are some discrepancies between bond orders calculated by ARCANA and bond lengths for example the C-O bond orders calculated for the complex are in reverse order to the trend in the experimental bond lengths (Table X).

This has been interpreted as due to the nature of ARCANA which depends on Lowdin delocalized atomic basis for obtaining self consistent charge distribution. Employing the Mulliken population analysis for obtaining the bond orders is probably not the best way, a new approach should be developed in this case.

Two configurations for the complex were calculated, the equilibrium configuration determined from X-ray data, in which the Cl-Pd-Cl axis is making $\sim 78^\circ$ with the plane containing the two pyridine rings. The other configuration is the symmetric one where the Cl-Pd-Cl axis is set perpendicular to the plane of the two rings.

The symmetric configuration was found to be stable electronically by about 0.142 a.u. This indicates that the stability of the established configuration is gained due to crystal packing effect, and not an electronic effect.

Acknowledgements

The authors acknowledge Kuwait University for provision of SC021 grant and Dr. Hayat Marafie for reviewing the manuscript.

References

- 1 N. M. Moussa, A. Laham, M. S. El-Ezaby, N. A. Al-Salem, M. E. Abu-Zeid, G. S. Mahmoud, A. Kabarity and S. Mazrooei, *Inorg. Biochem.*, **17**, 185 (1982).
- 2 F. Hanic, *Acta Crystallogr.*, **21**, 332 (1966).
- 3 A. Mosset, F. Nepveu-Juras, R. Haran and J. J. Bonnett, *J. Inorg. Nucl. Chem.*, **40**, 1259 (1978).
- 4 H. J. Franklin and F. M. Richardson, *Chem. Commun.*, **97** (1978).
- 5 J. Longo and M. F. Richardson, *Acta Crystallogr., Sect. B*, **36**, 2456 (1980).
- 6 D. M. Thompson, W. Balenovich, L. H. M. Hornich and M. F. Richardson, *Inorg. Chim. Acta*, **46**, 199 (1980).
- 7 'CAD4 operations manual', Enraf-Nonius, Delft, 1977.
- 8 D. T. Cromer and J. T. Waber, 'International Tables for X-ray Crystallography, Vol. IV', Kynoch Press, Birmingham, 1974, Table 2.2B.
- 9 J. A. Ibers and W. C. Hamilton, *Acta Crystallogr.*, **17**, 781 (1964).
- 10 D. T. Cromer and J. T. Waber, 'International Tables for

- X-ray Crystallography, Vol. IV', Kynoch Press, Birmingham, 1974, Table 2.3.1.
- 11 D. W. Cruickshank, *Acta Crystallogr.*, 2, 154 (1949).
 - 12 J. H. Corrington and L. C. Cusachs, *Int. J. Quantum Chem.*, 3S, 207 (1969).
 - 13 J. H. Corrington, H. S. Aldrich, C. W. McCurdy and L. C. Cusachs, *Int. J. Quantum Chem.*, 5, 307 (1971).
 - 14 J. J. Kaufman, H. J. T. Preston, E. Kerman and L. C. Cusachs, *Int. J. Quantum Chem.*, 7, 249 (1973).
 - 15 H. S. Aldrich, J. T. Mague and L. C. Cusachs, *Int. J. Quantum Chem.*, 7, 239 (1973).
 - 16 H. Basch, A. Viste and H. B. Gray, *Theor. Chim. Acta*, 3, 458 (1965).
 - 17 C. E. Moore, 'Atomic Energy Levels', Vol. III, National Bureau of Standards U.S. circular 467, 1958.
 - 18 C. F. Fischer, 'The Hartree-Fock Methods for Atoms', Wiley, New York, 1977.
 - 19 L. C. Cusachs and J. H. Corrington, in O. Sinanoglu and K. B. Wilber (eds.), 'Sigma Molecular Orbital Theory', Yale University Press, 1970, p. 256.
 - 20 R. H. B. Mais, P. G. Owston and M. A. Wood, *Acta Crystallogr., Sect. B*, 28, 2 (1972).
 - 21 R. C. Bingham, M. J. S. Dewar and D. H. Lo, *J. Am. Chem. Soc.*, 97, 1285 (1975).
 - 22 M. A. El-Dessouky, M. S. El-Ezaby and H. Abu Soud, *Inorg. Chim. Acta*, 106, 59 (1985).